Mechanistic Studies of Rat Protein Farnesyltransferase Indicate an Associative Transition State†

Chih-chin Huang,‡ Kendra E. Hightower,§ and Carol A. Fierke*

Department of Biochemistry, Box 3711, Duke University Medical Center, Durham, North Carolina 27710

Received October 11, 1999

ABSTRACT: Protein farnesyltransferase is a zinc metalloenzyme that catalyzes the transfer of a 15-carbon farnesyl group to a conserved cysteine residue of a protein substrate. Both electrophilic and nucleophilic mechanisms have been proposed for this enzyme. In this work, we investigate the detailed catalytic mechanism of mammalian protein farnesyltransferase by measuring the effect of metal substitution and/or substrate alterations on the rate constant of the chemical step. Substitution of cadmium for the active site zinc enhances peptide affinity approximately 5-fold and decreases the rate constant for the formation of the thioether product approximately 6-fold, indicating changes in the metal−thiolate coordination in the catalytic transition state. In addition, the observed rate constant for product formation decreases for C3 fluoromethyl farnesyl pyrophosphate substrates, paralleling the number of fluorines at the C3 methyl position and indicating that a rate-contributing transition state has carbocation character. Magnesium ions do not affect the affinity of either the peptide or the isoprenoid substrate but specifically enhance the observed rate constant for product formation 700-fold, suggesting that magnesium coordinates and activates the diphosphate leaving group. These data suggest that FTase catalyzes protein farnesylation by an associative mechanism with an "exploded" transition state where the metal-bound peptide/protein sulfur has a partial negative charge, the C1 of FPP has a partial positive charge, and the bridge oxygen between C1 and the α phosphate of FPP has a partial negative charge. This proposed transition state suggests that stabilization of the developing charge on the carbocation and pyrophosphate oxygens is an important catalytic feature.

Protein farnesyltransferase (FTase)[1] is a zinc metalloenzyme (*1*, *2*) that catalyzes the transfer of a 15-carbon farnesyl group from farnesyl pyrophosphate (FPP) to a conserved cysteine residue of the C-terminal "CaaX" motif of protein and peptide substrates (*3*, *4*). More than 30 farnesylated proteins have been identified in mammalian cells including Ras proteins, Rho proteins, nuclear lamins, and several proteins involved in visual signal transduction (*5*, *6*). Farnesylation of these proteins is required for membrane association and, possibly, interaction with other proteins (*3*, *6*). Since farnesylation is critical for the transformation of normal cells into cancerous cells by mutant forms of Ras, inhibitors of FTase are being investigated for antitumor activity (*5*, *7*, *8*).

Two distinct catalytic mechanisms have been proposed for FTase (Scheme 1): electrophilic (S_N1 or dissociative) with a carbocation at C1 of the FPP or nucleophilic (S_N2 or associative) with a thiolate at the cysteine residue of the CaaX motif. Evidence for electrophilic character in the transition state was obtained from the decreased steady-state turnover of yeast FTase when FPP substrate analogs substituted with fluorine, an electron-withdrawing group, at the C3 methyl position were utilized to destabilize the carbocation (*9*). Support for a nucleophilic mechanism comes from several observations including (1) direct coordination of the sulfur atom of the peptide substrate with the metal in FTase·isoprenoid·CaaX ternary complexes as observed by X-ray crystallography (*10*) and by optical absorbance spectroscopy of cobalt-substituted FTase (*11*), (2) the pH dependence of peptide binding, indicating that the peptide substrate is bound as the thiolate anion at physiological pH (*12*), (3) the inversion of configuration at C1 during catalysis (*13*, *14*), and (4) the secondary kinetic isotope effect near unity (*15*). Nucleophilic mechanisms have also been proposed for other zinc-containing enzymes and proteins that catalyze sulfur-alkylation reactions (*16*, *17*).

In this work, we further investigate the mechanism of mammalian FTase using transient kinetic studies of metal-

† This work was supported by National Institutes of Health Grant GM40602 (C.A.F.) and the Cancer Research Fund of the Damon Runyon-Walter Winchell Foundation Fellowship DRG-1450 (K.E.H.).

* To whom correspondence should be addressed at the Department of Chemistry, University of Michigan, 930 N. University, Ann Arbor, MI 48109-1055. Phone: (734) 936-2678. Fax: (734) 647-4865. E-mail: fierke@umich.edu.

‡ Current address: Department of Biochemistry and Biophysics, Texas A&M University, College Station, TX 77843.

§ Current address: Department of Biochemistry, Box 3686, Duke University Medical Center, Durham, NC 27710.

[1] Abbreviations: FTase, protein farnesyltransferase; FPP, farnesyl pyrophosphate; [^{3}H]FPP, tritium-labeled farnesyl pyrophosphate; TCEP, tris(2-carboxyethyl)phosphine hydrochloride; apo-FTase, FTase without bound metal; Zn-FTase, FTase with bound Zn^{2+}; Co-FTase, FTase with bound Co^{2+}; Cd-FTase, FTase with bound Cd^{2+}; Dns-GCVLS, dansylated pentapeptide Gly-Cys-Val-Leu-Ser; Heppso, *N*-[2-hydroxyethyl]-piperazine-*N*′-[hydroxypropanesulfonic acid]; TLC, thin layer chromatography; F_n-FPP; C3 mono-, di-, and trifluoromethyl farnesyl pyrophosphate analogs; GGTase-I, protein geranylgeranyltransferase type I.

10.1021/bi992356x CCC: $19.00
Published on Web 02/16/2000

Scheme 1. Reaction Catalyzed by FTase and Possible Transition States

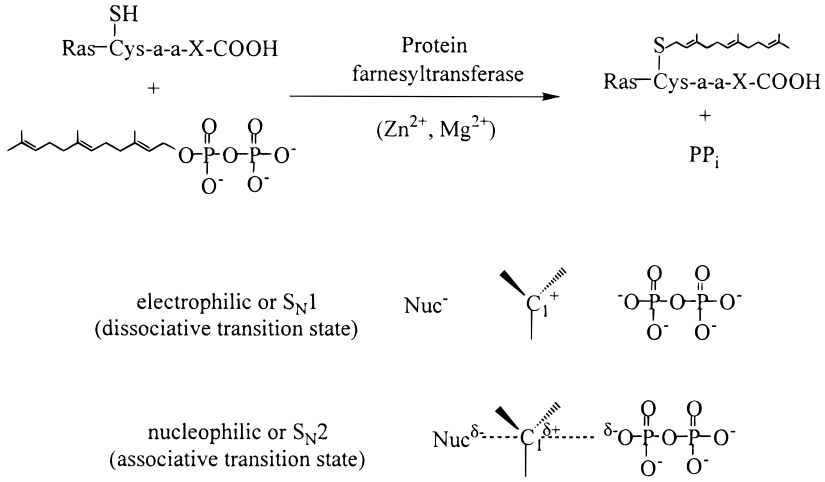

substituted FTase and FPP analogs. Substitution of the active site zinc with cadmium increases the affinity of the peptide substrate and decreases the rate constant for the chemical step, suggesting that the metal-coordinated substrate thiolate plays a nucleophilic role in catalysis. Removal of magnesium ions significantly decreases the rate constant for farnesylation without affecting substrate binding, consistent with the magnesium ion coordinating the pyrophosphate moiety of the substrate to stabilize the developing negative charge on the leaving group in the transition state. Finally, substitution of fluorine on the methyl group at the C3 position of FPP significantly decreases the rate constant for the chemical step, indicating that the transition state has carbocation character. These data suggest that the mechanism of FTase is associative with an "exploded" transition state where the bond to the pyrophosphate leaving group is nearly broken and the bond with the incoming thiolate nucleophile is barely formed.

EXPERIMENTAL PROCEDURES

Miscellaneous Methods. Tritium-labeled FPP ([^{3}H]FPP) and unlabeled FPP were purchased from American Radiolabeled Chemicals, Inc. (St. Louis, MO) or NEN LifeSciences (Boston, MA). Peptides (≥95% pure) were synthesized and HPLC-purified by Applied Analytical Industries (Chapel Hill, NC). Peptide concentrations were determined spectrophotometrically from the reaction of the cysteine with 5,5′-dithiobis(2-nitrobenzoic acid) (*18*, *19*). Protein concentrations were determined by the Coomassie Blue binding method (*20*) using a commercial kit (Bio-Rad). All assays were conducted at 25 °C. Unless otherwise stated, curve fitting was performed with KaleidaGraph (Synergy Software).

Preparation of Apo-FTase and Reconstitution with Metals. Recombinant rat FTase was overexpressed in *Escherichia coli* and purified as described previously (*21*). The zinc was removed from the enzyme (>1 mg/mL) by dialysis for 24 h at 4 °C against 50 mM Tris−HCl (pH 7.8), 1 mM tris(2-carboxyethyl)phosphine hydrochloride (TCEP), and 5 mM EDTA followed by an additional 24 h dialysis against 50 mM Tris−HCl (pH 7.8), 1 mM TCEP, and 50 μM EDTA (*11*). After dialysis, the apo-FTase was concentrated to greater than 50 μM, flash-frozen, and stored at -80 °C. FTase was reconstituted with Zn^{2+} (Zn-FTase), Co^{2+} (Co-FTase), or Cd^{2+} (Cd-FTase) by incubating the apo-enzyme (i.e., 100 μM enzyme, 50 μM EDTA) with the respective atomic absorption grade (Aldrich, Milwaukee, WI) metal salt (i.e., 150 μM) for 5−10 min on ice before dilution into the assay mixture.

Peptide Dissociation Constants. Dissociation constants for Dns-GCVLS were determined fluorimetrically, as described previously (*12*). The assays contained 20 nM FTase and 80 nM {(*E*,*E*)-2-[2-oxo-2-[[(3,7,11-trimethyl-2,6,10-dodecatrienyl)oxy]amino]ethyl]phosphonic acid, sodium} (Calbiochem, San Diego, CA), an inhibitory FPP analog, in 50 mM Heppso−NaOH (pH 7.8), ionic strength maintained at 0.1 M with NaCl, 1 mM TCEP, and 5 mM $MgCl_2$. For apo-FTase, the $MgCl_2$ was omitted and 200 μM EDTA was included in the assay. The data were fit to eq 1 if K_D > 3[FTase] or eq 2 if K_D < 3[FTase] (22), where ΔFL is the

$$\Delta FL = \frac{(EP - IF)}{(1 + K_D/[Dns])} + IF \quad (1)$$

$$\Delta FL = IF + \frac{(EP - IF)}{2[FTase]}[([FTase] + [Dns] + K_D) - [([FTase] + [Dns] + K_D)^2 - 4[FTase][Dns]]^{1/2}] \quad (2)$$

observed fluorescence after background subtraction, EP is the fluorescence end point, IF is the initial fluorescence, [Dns] is the concentration of Dns-GCVLS, and K_D is the dissociation constant for Dns-GCVLS.

Transient Kinetics with Metal-Substituted FTase. Single-turnover reactions contained 0.2 μM FTase, 0.1 μM [^{3}H]FPP (10 or 20 Ci/mmol), and 0.5−100 μM GCVLS or Dns-GCVLS in 50 mM Heppso−NaOH (pH 7.8) and 1 mM TCEP, with or without 5 mM $MgCl_2$. The residual EDTA concentration was less than 0.1 μM. The binary FTase•^{3}H-FPP complex was incubated for 5−10 min at 25 °C before the reaction was initiated by the addition of peptide. For assays performed in the absence of $MgCl_2$, 15 μL reactions were incubated for various times (5 s to 30 min) and then mixed with 15 μL of 60% 1-propanol, 1 mM HCl to stop the reaction. Assays containing 5 mM $MgCl_2$ (30 μL total volume) were carried out using a Kin-Tek rapid-quench apparatus and were quenched at various times (0.01−60 s) by the addition of 100 μL of 60% 1-propanol and 1 M HCl.

Product ([^{3}H]farnesylated GCVLS) was separated from substrate ([^{3}H]FPP or [^{3}H]farnesol if the stop solution was 60% 1-propanol, 1 M HCl) by thin-layer chromatography (TLC) on silica gel plates using a 6:3:1 (v/v/v) 1-propanol/NH_4OH/H_2O mobile phase (*23*). The ^{3}H-labeled substrates and products were visualized by autoradiography (24−48 h at −80 °C) following fluorographic enhancement (EN^{3}HANCE; NEN Life Science, Boston, MA). The product and substrate bands were excised from the plates, and the radioactivity was quantified by scintillation counting. The percentage of product formed was calculated from the ratio of radioactivity in the product band to the total radioactivity. The observed rate constant for product formation in the absence of magnesium was calculated using eq 3. For assays performed in the presence of magnesium, several data sets measured at varying peptide concentrations were fit simultaneously to eq 4 using Systat 5.2 (Systat, Inc.), where %P is the percent product at time t, EP is the percent product end point, k_1 is the peptide association rate constant, [GCVLS] is the concentration of peptide substrate, and k_2 is the observed rate constant for product formation.

$$\%P(t) = EP(1 - e^{-k_2 t}) \quad (3)$$

$$\%P(t) = EP\left[1 + \frac{1}{k_1[GCVLS] - k_2}(k_2 e^{-k_1[GCVLS]t} - k_1[GCVLS]e^{-k_2 t})\right] \quad (4)$$

Transient Kinetics with Apo-FTase. To determine the activity of apo-FTase in the presence and absence of 5 mM $MgCl_2$, the reactions were conducted in Zn-free glass vials (Fisher Scientific, Pittsburgh, PA) using solutions treated with Chelex-100 or EDTA. The FTase·^{3}H-FPP complex was preformed by incubating 10 μM apo-FTase with 5 μM [^{3}H]FPP (2 Ci/mmol) in 50 mM Heppso−NaOH (pH 7.8), 1 mM TCEP, and 200 μM EDTA (7.5 μL total assay volume). For reactions in the presence of magnesium, $MgCl_2$ (99.995%; Aldrich, Milwaukee, WI) was added to a final concentration of 5 mM after incubation of the apo-FTase with the [^{3}H]FPP. The reaction was initiated by the addition of GCVLS (10−100 μM) and quenched at various times (5 s to 2 h) with 7.5 μL of 2-propanol. Substrates and products were separated on silica gel TLC plates using a 8:1:1 (v/v/v) 2-propanol/NH_4OH/H_2O mobile phase and then processed as described above.

Steady-State Kinetics. Steady-state assays contained 24 nM FTase, 1 μM [^{3}H]FPP (10 Ci/mmol), and 10 μM GCVLS in 50 mM Heppso−NaOH (pH 7.8), 1 mM TCEP, and 5 mM $MgCl_2$ (7.5 μL total volume). For apo-FTase, 200 μM EDTA was included in the reaction. The reaction was initiated by the addition of FTase and quenched at various times (5 s to 1 h) with an equal volume of 2-propanol. The percentage of product formed was determined as described above using TLC and scintillation counting. The initial velocity was calculated from a linear fit of the first 10% of the reaction. Since both substrates are saturating, this value reflects the steady-state rate constant, k_{cat}.

Time-Dependent Absorption Spectra of Co-FTase. FPP analogs containing mono-, di-, or trifluoromethyl at the C3 position [F_n-FPP (*9*), Figure 1] were generously provided

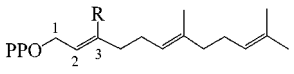

FPP R = CH_3

F_n-FPP
- F_1-FPP R = CH_2F
- F_2-FPP R = CHF_2
- F_3-FPP R = CF_3

FIGURE 1: Structures of C3 fluoromethyl FPP analogs (F_n-FPP) (*9*).

by Dr. C. Dale Poulter, University of Utah. Transient kinetics with these substrates were measured by the transient absorbance of the ligand−metal charge transfer band (340 nm) or the d−d transition band (635 nm) of Co-FTase (*11*). The Co-FTase·FPP or Co-FTase·F_n-FPP binary complexes (20 μM, 1:1 stoichiometry of enzyme to FPP or F_n-FPP) were mixed with 5 μM GCVLS, in 50 mM Heppso−NaOH (pH 7.8), 1 mM TCEP, and 5 mM $MgCl_2$ to initiate the reaction. For FPP and F_1-FPP, the reaction was monitored at 340 nm using a Kin-Tek stopped-flow spectrophotometer with a 2.5 cm path length. To measure rate constants for product formation using F_2-FPP and F_3-FPP as substrates, the time-dependent absorbance at 340 and 635 nm was measured using a Uvikon 9410 UV/vis double beam spectrophotometer. The reference cuvette contained the same concentration of Co-FTase·F_n-FPP used in the sample cuvette. The time-dependent changes in the absorbance were fit to an equation describing either two consecutive first-order reactions (FPP, eq 5) by nonlinear regression using the Marquat−Levenberg method provided in the Kin-Tek software package (*24*) or to a single first-order exponential (F_n-FPP, eq 6), where A is the absorbance at time t at the

$$A_{340}(t) = \Delta A_1 (e^{-k_1 t}) + \Delta A_2 (e^{-k_2 t}) + EP \quad (5)$$

$$A_{340\text{ or }635}(t) = \Delta A_2 (e^{-k_2 t}) + EP \quad (6)$$

specified wavelength, ΔA_1 is the change in absorbance due to peptide binding, k_1 is the rate constant for peptide association, ΔA_2 is the change in absorbance due to product formation, k_2 is the observed rate constant for product formation, and EP is the absorbance end point.

Product Formation with F_n-FPP and Dansylated Peptide. Single-turnover rate constants for product formation with Dns-GCVLS and F_n-FPP catalyzed by Zn- and Cd-FTase were measured using the fluorescence enhancement of the dansyl group (excitation at 340 nm, emission at 496 nm) of the peptide substrate upon product formation (*25*, *26*). The reaction was initiated by the addition of Dns-GCVLS (1 μM) to FTase·F_n-FPP (0.2 μM, 1:1 stoichiometry of FTase to F_n-FPP) in 50 mM Heppso−NaOH (pH 7.8), 1 mM TCEP, and 5 mM $MgCl_2$. The observed rate constant for product formation, k_2, was obtained by fitting the data to eq 7, where FL(t) is the fluorescence at time t, EP is the fluorescence end point, and IF is the initial fluorescence.

$$FL(t) = (EP - IF)(1 - e^{-k_2 t}) + IF \quad (7)$$

Measurement of FPP Affinity. FPP affinity was measured by equilibrium dialysis as described previously (*21*). The assay was performed in 50 mM Heppso−NaOH (pH 7.8) and 1 mM TCEP, with or without 5 mM $MgCl_2$. One

Table 1. Kinetic Values for Metal-Substituted FTase

	K_D (μM)[a]	k_1 (M^{-1} s^{-1})	k_2 (s^{-1})	k_2, $-Mg^{2+}$ (s^{-1})[b]	k_{cat} (s^{-1})
Zn-FTase	0.06 ± 0.003	$(5.5 \pm 0.6) \times 10^5$	12 ± 2	$(1.7 \pm 0.3) \times 10^{-2}$	$(2.2 \pm 0.1) \times 10^{-2}$
Co-FTase	0.09 ± 0.01	$(7.1 \pm 0.7) \times 10^5$	10 ± 4	$(1.5 \pm 0.8) \times 10^{-2}$	$(2.2 \pm 0.2) \times 10^{-2}$
Cd-FTase	0.012 ± 0.003	$(5.3 \pm 0.4) \times 10^5$	2 ± 0.4	$(1.7 \pm 0.4) \times 10^{-2}$	$(3.0 \pm 0.2) \times 10^{-2}$
apo-FTase	>10[b]	ND[c]	$<1 \times 10^{-4}$	$<1 \times 10^{-5}$	$(1.9 \pm 0.2) \times 10^{-4}$

[a] Peptide dissociation constants were measured with Dns-GCVLS. [b] These assays were performed without $MgCl_2$. [c] ND denotes not determined.

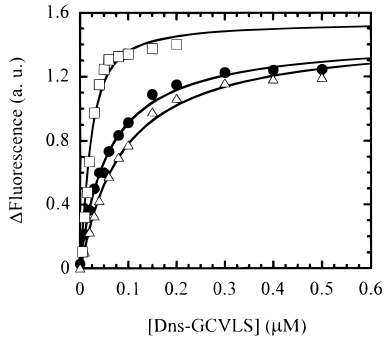

FIGURE 2: Peptide affinity of metal-substituted FTase. Dissociation constants were determined for Dns-GCVLS by direct titration of 20 nM metal-substituted FTase, 80 nM {(*E*,*E*)-2-[2-oxo-2-[[(3,7,11-trimethyl-2,6,10-dodecatrienyl)oxy]amino]ethyl]phosphonic acid, sodium} as described in the Experimental Procedures. The fluorescence emission was monitored at 496 nm after excitation at 280 nm. The plot shows peptide titrations for the binary complexes of Zn-FTase (●), Co-FTase (△), and Cd-FTase (□) after subtraction of Dns-GAVLS background. The K_D values were calculated from eq 1 (Zn-FTase and Co-FTase) or eq 2 (Cd-FTase) (see Table 1).

chamber contained 2−100 nM FTase (1 mL), while the other chamber contained 20 nM [^{3}H]FPP (20 Ci/mmol, 1 mL). The FPP dissociation constant, K_D, was obtained from eq 8,

$$\frac{[E\cdot FPP]}{[FPP]t} = \frac{EP}{1 + K_D/[E]_{free}} \quad (8)$$

where [E·FPP] is the concentration of enzyme-bound FPP, $[FPP]_t$ is the concentration of total FPP, EP is the maximal ratio of bound to total FPP, and $[E]_{free}$ is the concentration of free enzyme.

RESULTS

Affinity of Metal-Substituted FTase for Peptides. Zinc and cobalt are similar metals in both size (88 and 83 pm, respectively) and polarizability. Cadmium is a significantly larger (99 pm) and more polarizable metal than zinc and consequently has a higher affinity for coordination of sulfur atoms (*27*). Since the metal ion in FTase coordinates the substrate thiolate at physiological pH (*11*, *12*), substitution of the zinc with a more polarizable metal should lower the dissociation constant of the peptide. As expected, substitution of cobalt for the active site zinc does not greatly affect the dissociation constant of the peptide Dns-GCVLS (Figure 2, Table 1). However, the affinity of Cd-FTase for Dns-GCVLS or GCVLS (data not shown) is enhanced approximately 5-fold compared to that of Zn-FTase. This effect is somewhat smaller than that observed for small molecule complexes where cadmium generally coordinates thiolates 1-2 orders of magnitude more tightly than zinc (*28*−*30*). However, these model systems do not reflect a catalytic system where both a reactive thiolate and rapid product dissociation are required.

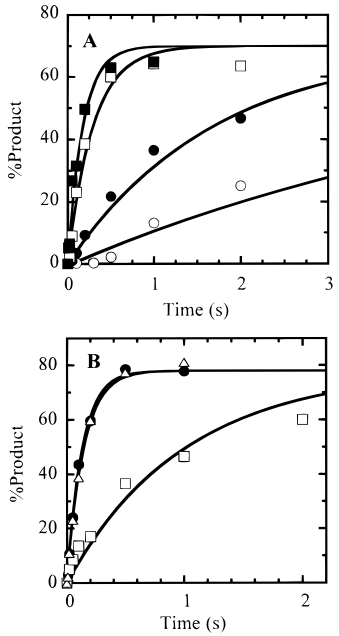

FIGURE 3: Product formation in the presence of $MgCl_2$. Single-turnover assays were performed as described in the Experimental Procedures with 0.2 μM enzyme, 0.1 mM[^{3}H]FPP, and 0.5−100 μM GCVLS in 50 mM Heppso−NaOH (pH 7.8), 1 mM TCEP, and 5 mM $MgCl_2$. (A) Product formation by Zn-FTase at 0.5 μM (○), 2 μM (●), 50 μM (□), and 100 μM (■) GCVLS peptide substrate. The peptide association rate constant, k_1, and the rate constant for product formation, k_2, were calculated from data collected at varying peptide concentrations using eq 4 (see Table 1). (B) Product formation by Zn-FTase (●), Co-FTase (△), and Cd-FTase (□) measured at 100 μM GCVLS.

Removal of the active site metal decreases the affinity of FTase for Dns-GCVLS more than 150-fold (Table 1), consistent with previous work suggesting that the bound zinc was required for peptide binding (*1*).

Effect of Metal Substitution on Product Formation. For mammalian FTase, substrate association and product dissociation, respectively, are the rate-limiting steps in steady-state turnover under conditions of subsaturating and saturating substrate (*31*, *32*). Therefore, neither of the steady-state rate constants, k_{cat} or k_{cat}/K_M, provides information about the transition state of the chemical step. To determine whether substitution of the active site metal affects the rate constant for the formation of the farnesylated peptide product, we measured product formation using transient kinetics to isolate the chemical step (Figure 3). We fit these data using an equation describing two consecutive, irreversible steps (eq 1) reflecting substrate association followed by farnesylation for the following reasons. Previous pre-steady-state kinetic studies of mammalian Zn-FTase in the presence of $MgCl_2$ indicated that the rate constant for association of the peptide substrate to the FTase·FPP binary complex is essentially irreversible, since the rate constant for farnesylation is faster than the rate constant for substrate dissociation

Scheme 2. Minimal Kinetic Scheme for FTase[a]

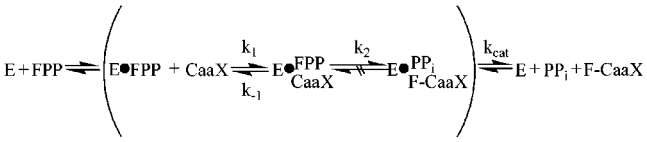

[a] The steps in parentheses are those that are measured by the single-turnover assays described in this paper. For this scheme, k_1 denotes the peptide association rate constant and k_2 is the rate constant for product formation (chemistry). For mammalian FTase, the steady-state rate constant, k_{cat}, is rate-limiting in the overall reaction (*31*, *32*).

($k_2 \gg k_{-1}$) (see Scheme 2; refs *11* and *31*). Consistent with this conclusion, the $K_{1/2}$ for the peptide concentration dependence of the single-turnover farnesylation rate constant for Zn-, Co-, and Cd-FTase are calculated as 20, 14, and 6 μM, respectively, assuming a rapid equilibrium mechanism ($k_2 \ll k_{-1}$) (Figure 3A). These values are significantly higher than the direct measurements of the affinity of an FTase•isoprenoid binary complex for the peptide substrate, suggesting that the $K_{1/2}$ does not reflect K_D but rather reflects a change in rate-limiting steps from substrate binding to farnesylation as the concentration of peptide increases. The measured values of k_2 are comparable to previous values measured under single-turnover conditions using the peptide TKCVIM (*11*) or by fluorescence changes using a biotinylated GLPCVVM peptide (*31*) but are significantly faster than a recent pre-steady-state measurement for farnesylation of a biotinylated KKSKTKCVIM peptide (*33*).

To test whether a metal-bound thiolate plays a nucleophilic role in the catalytic transition state of FTase, we investigated whether changing the characteristics of the metal−thiolate interaction affects the free energy of the transition state. Increasing the strength of the metal−thiolate interaction should lower the pK_a and nucleophilicity of the metal-bound thiolate, thereby decreasing the rate constant for nucleophilic reactions (*34*, *35*). The observed rate constant for product formation, k_2, for Zn-FTase is 12 ± 2 s^{-1} (Figure 3B, Table 1). As expected, substitution of the active site zinc with cobalt has little effect on k_2. However, k_2 is 6-fold lower for Cd-FTase (2 ± 0.4 s^{-1}) when compared to Zn-FTase, suggesting that a metal-bound nucleophile is involved in catalysis. These effects of metal substitution on k_2 parallel the measured changes in the pK_a of the metal-bound thiolate where cobalt substitution has no effect and cadmium substitution decreases the pK_a by approximately 1 pH unit (*12*, M. J. Saderholm and C. A. Fierke, unpublished result). Cadmium substitution experiments performed with the *E. coli* repair protein Ada (*36*), cobalamin-dependent methionine synthase (*37*), and betaine−homocysteine methyltransferase (*38*), zinc metalloproteins which also alkylate sulfur groups, show similar decreases in their reaction rates.

Substitution of cadmium for zinc in FTase has little effect on other steps in the kinetic pathway, suggesting that this change does not cause major alterations in the active site structure. The association rate constant, k_1, for peptide substrate binding to the FTase•FPP binary complex is rapid ($(5-7) \times 10^5$ M^{-1} s^{-1}, Table 1), not dependent on the nature of the metal ion at the active site, and consistent with previously reported values (*11*, *31*). Therefore, the observed decrease in the peptide K_D for Cd-FTase reflects a slower dissociation rate constant. Additionally, the steady-state rate constant, k_{cat}, for FTase is not altered by substitution of the zinc by either cobalt or cadmium, indicating that metal coordination of the farnesylated peptide product does not limit product dissociation (Table 1).

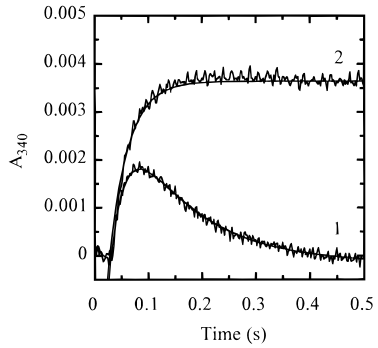

FIGURE 4: Reactivity of Co-FTase with fluoromethyl FPP analogs. The transient absorbance was measured at either 340 or 635 nm after mixing 20 μM Co-FTase•FPP or Co-FTase•F_n-FPP (1:1 stoichiometry of enzyme to FPP or F_n-FPP) with 4 μM GCVLS in 50 mM Heppso−NaOH (pH 7.8), 1 mM TCEP, and 5 mM $MgCl_2$. The plot shows time courses for the reaction of Co-FTase•FPP (line 1) and Co-FTase•F_2-FPP (line 2). The data were fit to eq 5 (FPP) or eq 6 (F_n-FPP) to calculate k_1 and k_2.

Fluoromethyl FPP Analogs. The F_n-FPP analogs contain fluorine substitutions on the methyl group at the C3 position of FPP (Figure 1, ref *9*). The fluorine is electron withdrawing and destabilizes development of positive charge at the C1 position in the transition state, resulting in a decrease in the observed rate constant for product formation in electrophilic reactions. Previously, Dolence and co-workers have shown that steady-state turnover catalyzed by yeast FTase is decreased significantly for fluorine-substituted FPP substrates (*9*). However, product release is partially rate-limiting for yeast FTase (*39*) so the decreased activity may not directly correlate with destabilization of the transition state for farnesylation. Since product release is also rate-limiting for mammalian FTase under steady-state conditions (*31*, *32*), we used transient kinetics to study the influence of fluorine substitution on the transition state for farnesylation in FTase.

The effects of fluoromethyl substitution at the C3 position of FPP on the reaction catalyzed by Co-FTase were determined by transient absorbance spectroscopy under single-turnover conditions (Figure 4). These data are biphasic. The first phase, marked by an increase in the cobalt−thiolate charge transfer band at 340 nm, monitors the binding of the peptide to the enzyme-bound metal. The second-order rate constant for peptide binding calculated from this phase is approximately 1×10^6 M^{-1} s^{-1} for all of the Co-FTase•F_n-FPP complexes, suggesting that the fluorine substitutions do not affect the association of the peptide with the enzyme. The second phase, characterized by a decrease in the 340 nm absorbance, measures product formation (*11*). Using FPP and F_1-FPP, the single-turnover rate constants were determined to be 8.8 ± 0.5 and 0.22 ± 0.06 s^{-1}, respectively (Table 2). For F_2-FPP and F_3-FPP, product formation was monitored by absorbance changes at 635 nm, indicative of the geometry of the enzyme-bound cobalt ion, since the background absorbance at 340 nm slowly decreased. The rate constant for the chemical step decreases with each additional fluorine, resulting in a 40-fold decrease in k_2 for F_1-FPP, a 600-fold decrease for F_2-FPP, and an almost 3000-fold decrease for F_3-FPP compared to that for FPP. These decreases are somewhat larger than the data previously

Table 2: Effect of Fluorine and Metal Substitution on the Observed Rate Constant of Product Formation

	peptide substrate		isoprenoid substrate[a]			
			FPP	F_1-FPP	F_2-FPP	F_3-FPP
Zn-FTase	Dns-GCVLS	k_2 (s^{-1})	4.2 ± 0.4	$(7.7 \pm 1.0) \times 10^{-2}$	$(1.2 \pm 0.2) \times 10^{-2}$	$(1.1 \pm 0.4) \times 10^{-3}$
		k_{rel}[b]	1	1.8×10^{-2}	2.7×10^{-3}	2.6×10^{-4}
Co-FTase	Dns-GCVLS	k_2 (s^{-1})	3.5 ± 0.4			
	GCVLS	k_2 (s^{-1})	8.8 ± 0.5	0.22 ± 0.06	$1.4 \pm 0.5 \times 10^{-2}$	$3.0 \pm 1.0 \times 10^{-3}$
		k_{rel}[b]	1	2.5×10^{-2}	1.6×10^{-3}	3.4×10^{-4}
Cd-FTase	Dns-GCVLS	k_2 (s^{-1})	1.7 ± 0.2	$(5.9 \pm 1.8) \times 10^{-2}$	$(1.0 \pm 0.3) \times 10^{-2}$	$(1.3 \pm 0.7) \times 10^{-3}$
		k_{rel}[b]	1	3.5×10^{-2}	6.1×10^{-3}	7.4×10^{-4}

[a] Fluorine substitution is on the methyl group on carbon 3 of the farnesyl chain (Figure 1). [b] The observed rate constant for product formation with FPP was taken as 1 for each metal-substituted FTase.

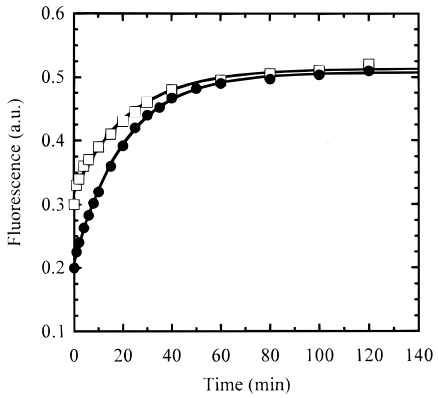

FIGURE 5: Measurement of the rate constant of the chemical step with Dns-GCVLS. The assays were performed with 0.2 μM FTase·F_n-FPP, 1 μM Dns-GCVLS in 50 mM Heppso−NaOH (pH 7.8), 1 mM TCEP, and 5 mM $MgCl_2$. The fluorescence emission of the dansyl group was monitored at 496 nm after excitation at 340 nm. The plot shows data for the reaction of Zn-FTase (●) and Cd-FTase (□) with F_3-FPP. The observed rate constants for product formation were calculated using eq 7 (see Table 2).

obtained for yeast FTase (*9*) and indicate that the transition state of rat FTase has significant carbocation character.

The previous sets of experiments suggest that the mechanism of catalysis of rat FTase is concerted with both electrophilic and nucleophilic characteristics. To further test this hypothesis, we investigated the effect of metal substitution on the single-turnover rate constant for product formation using the fluoromethyl FPP analogs. If the mechanism is concerted, substitution of the more polarizable cadmium for the zinc or cobalt should have an additive effect on the observed rate constant of product formation with the fluoromethyl analogs, resulting in a greater decrease in k_2. This experiment is similar to multiple isotope experiments that have been used extensively to distinguish a concerted mechanism from a stepwise mechanism (*40*−*43*) by combining isotopes which test each potential step in the transition state. If the mechanism is concerted, the effects of the multiple isotopes should be additive. Changes in the fluorescence of Dns-GCVLS upon product formation were used to determine k_2 for Zn- and Cd-FTase (Figure 5). Contrary to the expected result for a concerted mechanism, the effect of cadmium substitution on k_2 decreases for the fluoromethyl FPP analogs from a Zn-FTase/Cd-FTase ratio of 2.5 for FPP to approximately 1 for F_2-FPP and F_3-FPP (Table 2). These data indicate that the rate-limiting transition state for the fluorinated analogs is altered with less dependence on the nucleophilicity of the metal−thiolate. This behavior could potentially indicate that destabilization of the carbocation by fluorine causes the transition state to occur earlier on the reaction pathway (*44*). Alternatively, the multiple alterations in the substrate (F_n-FPP and Dns-GCVLS) and enzyme (Cd-FTase) could significantly alter the reaction pathway. The details of the transition-state structure in FTase will need to be reexamined using multiple isotope effect experiments where the alterations in the substrate structures are less extensive.

Influence of Magnesium on Product Formation. In addition to enzyme-bound zinc, millimolar concentrations of magnesium are required for optimal activity of FTase under steady-state conditions (*1*, *45*). The maximal observed rate constant for product formation under single-turnover conditions is also achieved when ≥10 mM magnesium is present in the assay (M. J. Saderholm and C. A. Fierke, unpublished results). However, a slow rate of product formation is observed even in the absence of magnesium (Table 1). This rate constant is unaffected by procedures that decrease any potential magnesium contamination, such as treatment of buffers with Chelex, addition of the metal chelator EDTA, and use of metal-free reaction vials (see the Experimental Procedures). The k_2 for product formation in the absence of magnesium, approximately 1.7×10^{-2} s^{-1} irrespective of the metal at the active site (Table 1), is decreased 700-fold for Zn- and Co-FTase and 120-fold for Cd-FTase compared to the reaction containing Mg^{2+}. Nonetheless, this k_2 is significantly higher than that of the measured background reaction for apo-FTase. These data demonstrate that magnesium accelerates a step at or before formation of the transition state for farnesylation. However, the absence of an effect of cadmium substitution on k_2 suggests an alteration in either the structure of the transition state or the rate-limiting step for formation of the thioether product in the absence of magnesium.

To determine whether magnesium influences the formation of the ternary complex, the effect of magnesium on substrate binding was studied. Previous work suggested that magnesium was not required for FPP binding (*1*). The dissociation constants for FPP (Figure 6) were determined to be 6.5 ± 1.7 nM in the presence (*21*) and 5.2 ± 1.2 nM in the absence of 5 mM $MgCl_2$, indicating that the affinity of FPP for FTase is not affected by magnesium under these conditions. These values are similar to previous FPP dissociation constants measured in the presence of magnesium (*31*, *46*). Similarly, magnesium does not affect the affinity of peptides for a binary complex containing an inhibitory FPP analog (*12*). Finally, the association rate constant for GCVLS with the Co-FTase·FPP complex, measured by transient absorption spectra, was determined to be 8.5×10^5 M^{-1} s^{-1} in the absence of magnesium (data not shown), which is similar to

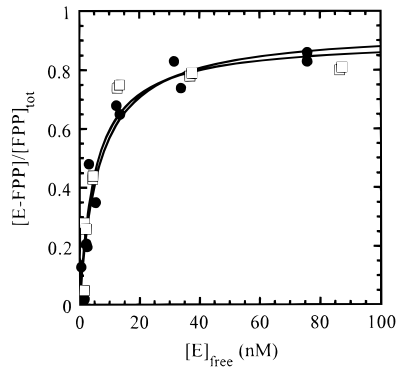

FIGURE 6: Effect of magnesium on the FPP dissociation constant. The FPP dissociation constants was determined using equilibrium dialysis as described in the Experimental Procedures with 2-100 nM Zn-FTase and 20 nM [^{3}H]FPP in 50 mM Heppso−NaOH (pH 7.8) and 1 mM TCEP, with or without 5 mM $MgCl_2$. The calculated dissociation constants (eq 8) are 6.5 ± 1.7 (*21*) and 5.2 ± 1.2 nM in the presence (●) and absence (□), respectively, of magnesium.

the association rate constant measured in the presence of magnesium (Table 1, ref *11*). These data indicate that magnesium has little or no effect on the formation of the ternary FTase·FPP·peptide complex but significantly enhances the rate constant of a step after formation of the ternary complex and at or before the chemical step.

DISCUSSION

Zinc−Thiolate Nucleophile. For zinc−metalloenzymes, substitution of the zinc by other metals can provide important information about the zinc coordination sphere and its involvement in catalysis. Previously, Co^{2+}-substituted FTase has been used to demonstrate that the peptide cysteine is directly coordinated to the metal (*11*) and that the pK_a of the thiol is lowered by interaction with the metal (*12*). These studies suggest that the zinc in FTase is directly involved in the catalytic mechanism, consistent with the direct zinc−sulfur coordination observed in the X-ray crystal structure of a FTase ternary complex containing the peptide substrate acetyl-CVIselenoM and an inhibitory FPP analog, α-hydroxyfarnesylphosphonic acid (*10*). A more direct assessment of the role of the zinc ion in catalysis can be explored by substitution of the zinc with cadmium. Cadmium is a more thiophilic metal than zinc and cobalt (*27*) and should consequently have a stronger interaction with the peptide cysteine thiolate. This increased interaction should be manifest as a tighter dissociation constant for the peptide, as observed (Table 1). Furthermore, the pK_a of the metal-bound peptide thiol decreases for the cadmium-substituted enzyme (M. J. Saderholm and C. A. Fierke, unpublished data), consistent with enhanced cadmium−thiolate coordination in the ground state. However, the observed 5-fold increase in affinity is less than the 10−100-fold enhancement for thiolate coordination by cadmium in small molecule complexes (*28*−*30*). These data suggest that the metal−thiolate coordination in FTase·peptide complexes is suboptimal, consistent with the long (2.5 Å) metal−thiolate distance observed in the X-ray crystal structure (*10*).

The enhancement of peptide affinity in cadmium-substituted FTase may explain the altered peptide specificity under steady-state conditions observed for Cd-FTase (*47*) and cadmium-substituted protein geranylgeranyltransferase type I (GGTase-I; ref *48*), which catalyzes a reaction similar to FTase and probably has a similar catalytic mechanism. A general increase in peptide affinity due to enhanced metal−thiolate coordination would have little effect on the $k_{cat}/K_M^{peptide}$ for peptide substrates where peptide association is essentially irreversible and occurs at a diffusion-controlled rate constant ($k_{off}^{peptide} < k_{chemistry}$), as observed for a biotinylated GLPCVVM peptide (*31*). However, for more weakly bound peptides a decrease in $K_D^{peptide}$ would cause an increase in $k_{cat}/K_M^{peptide}$. These alterations in the microscopic rate constants would be observed as a net reduction in the peptide specificity of the enzyme.

A weak metal−thiolate bond in the FTase·peptide complexes might be an important catalytic feature as this should increase the pK_a and enhance the nucleophilicity of the bound thiolate. Consistent with this proposal, the reactivity of the peptide decreases in the more tightly bound Cd-FTase complex. In fact, for cadmium substitution the decrease in the farnesylation rate constant parallels both the decrease in the metal−thiol pK_a and the increase in peptide affinity. These data could be described simply as stabilization of the ground-state FTase·FPP·peptide complex by 1 kcal/mol relative to FTase·FPP with no alteration in the energy of the transition state. This hypothesis is consistent with model studies mimicking the *E. coli* DNA repair protein Ada, a zinc−metalloprotein that facilitates a sulfur-alkylation reaction similar to FTase, which suggests that alkylation of metal−thiolate coordination complexes occurs via a dissociated thiolate (*49*). However, the visible spectrum of Co-FTase with bound farnesylated product is consistent with metal−thioether coordination (*11*), and similar metal coordination of a thioether product has been suggested for Ada (*50*, *51*). Taken together these data suggest that a metal-assisted nucleophile is involved in the catalytic mechanism of FTase.

Transition State Structure. Previously, the decreased turnover of fluorine-substituted FPP catalyzed by yeast FTase suggested an electrophilic component in the rate-limiting transition state of this enzyme (*9*). Using transient kinetics, the electrophilic character of the transition state for farnesylation catalyzed by mammalian FTase was investigated. Fluorine substitution at the C3 methyl decreases the rate constant for the chemical step, suggesting that the transition state has substantial carbocation character. The decreases in reactivity caused by fluorine substitution in both mammalian and yeast FTase are significantly smaller than the effects of fluorine substitution on either the solvolysis of dimethylallyl *p*-methoxybenzenesulfonates or the reactivity of farnesyl pyrophosphate synthase, which both proceed via an electrophilic reaction (*9*, *52*). The effects of the fluorine substitution on FTase reactivity more closely parallel the effects on solvolysis reactions in the presence of a potent nucleophile such as azide, which proceed via an associative mechanism with an "exploded" transition state (*53*, *54*). This correlation suggests a similar transition-state structure in FTase.

These fluoromethyl FPP analog experiments (Tables 1 and 2; ref *9*) indicate the existence of carbocation character in the transition state. However, the magnitude of this effect as well as the dependence of the farnesylation rate constant on the nucleophilicity of the metal−thiolate suggests that the transition state of FTase has associative character. Additionally, the inability to trap a carbocation intermediate by reaction with water (farnesol product) or added ^{32}P-labeled

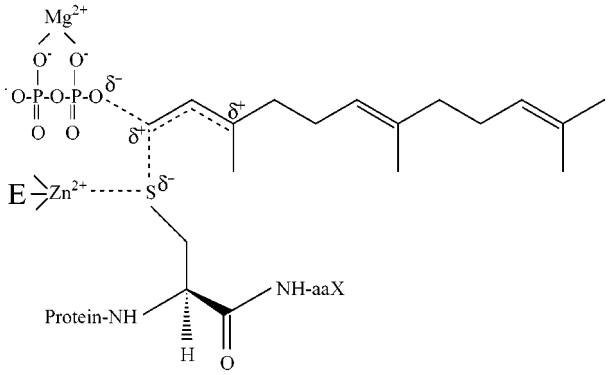

FIGURE 7: Proposed transition state of FTase. The results detailed here and in previous studies (*9*−*15*, *33*) suggest that the transition state of FTase is associative with a partial positive charge on C1 of FPP and partial negative charges on the peptide sulfur and the bridge oxygen between C1 and the α phosphate of FPP. The magnesium is shown coordinated to the nonbridging pyrophosphate oxygens. E denotes the FTase zinc ligands, and the dashed lines represent partial bonds. Adapted from ref *17*.

pyrophosphate under any reaction conditions (C.-c. Huang and C. A. Fierke, unpublished data) also argues against the formation of a stable carbocation intermediate (*55*). A proposed associative transition state is shown in Figure 7 where the metal-bound peptide/protein sulfur has a partial negative charge and the C1 of FPP has a partial positive charge. This associative transition state is also consistent with other properties of the reaction catalyzed by FTase, including (1) the metal−thiolate coordination observed in ground-state FTase•isoprenoid•peptide complexes (*10*, *11*), (2) the inversion of configuration at the C1 carbon (*13*, *14*), (3) an α-secondary kinetic isotope effect near unity (*15*); (4) the spectral properties of the bound farnesylated product (*11*), and (5) the properties of mutants in the FTase active site at positions Y300*β* and K164α (*33*, *56*, *57*). However, the details of the transition-state structure remain to be determined using additional structure−reactivity correlations and isotope effect studies.

The structure of this proposed transition state (Figure 7) compared to the ground-state structure suggests potential mechanisms that FTase may use to selectively stabilize this transition state and, hence, catalyze farnesylation. In particular, stabilization of the developing negative charge on the pyrophosphate oxygens should stabilize this transition state. The largest increase in negative charge occurs on the bridge oxygen between C1 and the α phosphate of FPP, while the charge on the nonbridging oxygens on the α phosphate on FPP also increases (*58*, *59*). Strengthening hydrogen-bonding interactions with the bridging oxygen in the transition state would be one stabilization mechanism, as has been proposed recently for Ras-catalyzed hydrolysis of GTP (*59*). Residue H248*β*, which forms a 2.7 Å hydrogen bond with the bridge oxygen between C1 and the α phosphate of FPP in a modeled ternary complex (*10*, *33*), is a reasonable group to fulfill this function. However, mutations at position 248 appear to have small effects on catalysis (*33*, *56*). Potentially, other groups could interact with this bridging oxygen in the transition state. In the crystal structure a 7 Å distance is observed between the C1 of FPP and the cysteine thiolate (*10*), which is likely overcome by a conformational change to form an active complex. The increased charge on the nonbridging oxygens on the α phosphate on FPP could be stabilized in the transition state by interactions with the side chain of K164α. This group is within hydrogen-bonding distance of an α phosphate oxygen, and mutagenesis studies suggest that K164α stabilizes the farnesylation transition state (*33*).

Role of Magnesium. The role of magnesium in the reaction catalyzed by FTase has not yet been clearly established. While magnesium is not essential for catalysis by FTase, both single-turnover (Table 1) and steady-state reactions (*1*, *45*) are enhanced several orders of magnitude by millimolar concentrations of magnesium. Transient kinetics have confined the activation of FTase by magnesium to a step or steps at or before chemistry but after formation of the ternary complex, consistent with a proposal that magnesium coordinates the nonbridging pyrophosphate oxygens (Figure 7) to activate the diphosphate moiety as a leaving group. Magnesium ions bind to pyrophosphate 1−2 orders of magnitude more tightly than to prenyl diphosphates and hence should stabilize the formation of the pyrophosphate product and pyrophosphate-like transition state (*60*, *61*). In fact, divalent metal ions enhance the solvolysis of prenyl diphosphates by a comparable amount (*62*−*64*). Furthermore, in the isoprenoid synthases and transferases, which also use prenyl diphosphates as substrates, a magnesium ion polarizes and activates the pyrophosphate leaving group to facilitate formation of a carbocation intermediate (*65*−*68*). This catalytic magnesium ion binds to an aspartate-rich region on the protein and coordinates the pyrophosphate oxygens in the bound complex. However, in the structure of FTase there is no conserved asparate-rich region (*69*, *70*) and no evidence that magnesium binds to the enzyme in the absence of the substrate, suggesting that magnesium interacts mainly with the FPP substrate. In fact, coordinated magnesium ions may displace side chains that form hydrogen bonds with the phosphate oxygens in the absence of Mg(II) (*10*). Therefore, a possible alternative explanation consistent with the transient kinetic data is that the magnesium ion stabilizes the formation of an active ternary substrate complex with the C1 of FPP near the metal−thiolate. In light of these findings the report that the steady-state reaction catalyzed by GGTase-I may not be dependent upon magnesium for maximal activity is intriguing (*48*), perhaps suggesting significant alterations in the reaction mechanism of these related enzymes. A comparison of the catalytic role of magnesium in the FTase and GGTase-I will provide further insight into the mechanisms of these enzymes.

Zinc-Catalyzed Sulfur Alkylation. A variety of metalloproteins catalyze the alkylation of sulfur groups including the *E. coli* DNA repair protein Ada (*71*, *72*), cobalamin-dependent (*37*, *73*) and cobalamin-independent (*74*) methionine synthase, human betaine−homocysteine methyltransferase (*38*), methanol−coenzyme M methyltransferases (*75*, *76*), and FTase and the related prenylation enzymes GGTase-I (*45*) and protein geranylgeranyltransferase type II (*77*). For all of these enzymes, a metal-bound thiolate has been suggested as the nucleophile in the chemical step. However, FTase is the only member of this class of metalloproteins for which an electrophilic transition state has been implicated; in all of the other cases, the potential carbocation is significantly less stable than the allylic cation. The transition states of these enzymes likely are more associative and the reaction is more dependent on the

reactivity of the metal−thiolate. Model compounds that mimic the zinc binding site of Ada have suggested that increased coordination of the zinc by negatively charged thiolate groups correlates with decreased zinc−thiolate affinity (*78*). This weaker metal coordination should enhance the nucleophilicity of the bound thiolate. Consistent with this proposal, the majority of the metalloproteins that catalyze sulfur alkylation have at least two cysteine ligands (*17*). A comparison of the transition-state structure and structure−reactivity parameters of these related enzymes will provide a better understanding of the essential catalytic features of zinc-catalyzed sulfur alkylation.

ACKNOWLEDGMENT

We thank Dr. C. Dale Poulter and Dr. Dave Rozema for their generous gift of the fluorinated FPP analogs, and Dr. Hua-Wen Fu, Dr. Rebecca Spence, Dr. Matthew Saderholm, and Dr. Patrick Casey for assistance and helpful discussions.

REFERENCES

1. Reiss, Y., Brown, M. S., and Goldstein, J. L. (1992) *J. Biol. Chem. 267*, 6403−6408.
2. Chen, W.-J., Moomaw, J. F., Overton, L., Kost, T. A., and Casey, P. J. (1993) *J. Biol. Chem. 268*, 9675−9680.
3. Zhang, F. L., and Casey, P. J. (1996) *Annu. Rev. Biochem. 65*, 241−269.
4. 4. Casey, P. J., and Seabra, M. C. (1996) *J. Biol. Chem. 271*, 5289−5292.
5. Cox, A. D., and Der, C. J., (1997) *Biochim. Biophys. Acta 1333*, F51−F71.
6. Schafer, W. R., and Rine, J. (1992) *Annu. Rev. Genet. 30*, 209−237.
7. Leonard, D. M. (1997) *J. Med. Chem. 40*, 2971−2990.
8. Sebti, S. M., and Hamilton, A. D. (1997) *Pharmacol. Ther. 74*, 103−114.
9. Dolence, J. M., and Poulter, C. D. (1995) *Proc. Natl. Acad. Sci. U.S.A. 92*, 5008−5011.
10. Strickland, C. L., Windsor, W. T., Syto, R., Wang, L., Bond, R., Wu, Z., Schwartz, J., Le, H. V., Beese, L. S., and Weber, P. C. (1998) *Biochemistry 37*, 16601−16611.
11. Huang, C.-c., Casey, P. J., and Fierke, C. A. (1997) *J. Biol. Chem. 272*, 20−23.
12. Hightower, K. E., Huang, C.-c., Casey, P. J., and Fierke, C. A. (1998) *Biochemistry 37*, 15555−15562.
13. Mu, Y., Omer, C. A., and Gibbs, R. A. (1996) *J. Am. Chem. Soc. 118*, 1817−1823.
14. Edelstein, R. L., Weller, V. A., Distefano, M. D., and Tung, J. S. (1998) *J. Org. Chem. 63*, 5298−5299.
15. Weller, V. A., and Distefano, M. D. (1998) *J. Am. Chem. Soc. 120*, 7975−7976.
16. Matthews, R. W., and Goulding, C. W. (1997) *Curr. Opin. Chem. Biol. 1*, 332−339.
17. Hightower, K. E., and Fierke, C. A. (1999) *Curr. Opin. Chem. Biol. 3*, 176−181.
18. Ellman, G. L. (1959) *Arch. Biochem. Biophys. 82*, 70−77.
19. Riddles, P. W., Blakeley, R. L., and Zerner, B. (1979) *Anal. Biochem. 94*, 75−81.
20. Bradford, M. M. (1976) *Anal. Biochem. 72*, 248−254.
21. Zimmerman, K. K., Scholten, J. D., Huang, C.-c., Fierke, C. A., and Hupe, D. J. (1998) *Protein Exp. Purif. 14*, 395−402.
22. Segel, I. H. (1975) *Enzyme Kinetics*, pp 72−74, John Wiley and Sons, New York.
23. Goldstein, J. L., Brown, M. S., Stradley, S. J., Reiss, Y., and Gierasch, L. M. (1991) *J. Biol. Chem. 266*, 15575−15578.
24. Johnson, K. A. (1986) *Methods Enzymol. 134*, 677−705.
25. Pompliano, D. L., Gomez, R. P., and Anthony, N. J. (1992) *J. Am. Chem. Soc. 114*, 7945−7946.
26. Cassidy, P. B., Dolence, J. M., and Poulter, C. D. (1995) *Methods Enzymol. 250*, 30−43.
27. Pearson, R. G. (1963) *J. Am. Chem. Soc. 85*, 3533−3539.
28. Li, N. C., and Manning, R. A. (1955) *J. Am. Chem. Soc. 77*, 5225−5228.
29. Martin, R. B., and Edsall, J. T. (1959) *J. Am. Chem. Soc. 81*, 4044−4047.
30. Knoblock, E. C., and Purdy, W. C. (1961) *Radiat. Res. 15*, 94−96.
31. Furfine, E. S., Leban, J. J., Landavazo, A., Moomaw, J. F., and Casey, P. J. (1995) *Biochemistry 34*, 6857−6862.
32. Tschantz, W. R., Furfine, E. S., and Casey, P. J. (1997) *Biochemistry 272*, 9989−9993.
33. Wu, Z., Demma, M., Strickland, C. L., Radisky, E. S., Poulter, C. D., Le, H. V., and Windsor, W. T. (1999) *Biochemistry 38*, 11239−11249.
34. Fersht, A. (1985) *Enzyme Structure and Mechanism*, 2nd ed., pp 47−90, W. H. Freeman and Company, New York.
35. Dahl, K. H., and McKinley-McKee, J. S. (1981) *J. Inorg. Biochem. 15*, 79−87.
36. Myers, L. C., Jackow, F., and Verdine, G. L. (1995) *J. Biol. Chem. 270*, 6664−6670.
37. Goulding, C. W., and Matthews, R. G. (1997) *Biochemistry 36*, 15749−15757.
38. Millian, N. S., and Garrow, T. A. (1998) *Arch. Biochem. Biophys. 356*, 93−98.
39. Mathis, J. R., and Poulter, C. D. (1997) *Biochemistry 36*, 6367−6376.
40. Hermes, J. D., Roeske, C. A., O'Leary, M. H., and Cleland, W. W. (1982) *Biochemistry 21*, 5106−5114.
41. Hermes, J. D., Tipton, P. A., Fisher, M. A., O'Leary, M. H., Morrison, J. F., and Cleland, W. W. (1984) *Biochemistry 23*, 6263−6275.
42. Belasco, J. G., Albery, W. J., and Knowles, J. R. (1986) *Biochemistry 25*, 2552−2558.
43. O'Keefe, S. J., and Knowles, J. R. (1986) *Biochemistry 25*, 6077−6084.
44. Jencks, W. P. (1985) *Chem. Rev. 85*, 511−527.
45. Moomaw, J. F., and Casey, P. J. (1992) *J. Biol. Chem. 267*, 17438−17443.
46. Pompliano, D. L., Schaber, M. D., Mosser, S. D., Omer, C. A., Schaber, J. A., and Gibbs, J. B. (1993) *Biochemistry 32*, 8341−8347.
47. Zhang, F. L, Fu, H.-W., Casey, P. J., and Bishop, W. R. (1996) *Biochemistry 35*, 8166−8171.
48. Zhang, F. L., and Casey, P. J. (1996) *Biochem. J. 320*, 925−932.
49. Wilker, J. J., and Lippard, S. J. (1997) *Inorg. Chem. 36*, 969−978.
50. Myers, L. C., Cushing, T. D., Wagner, G., and Verdine, G. L. (1994) *Chem. Biol. 1*, 91−97.
51. Ohkubo, T., Sakashita, H., Sakuma, T., Kainosho, M., Sekiguchi, M., and Morikawa, K. (1994) *J. Am. Chem. Soc. 116*, 6035−6036.
52. Poulter, C. D., Wiggins, P. L., and Le, A. T. (1981) *J. Am. Chem. Soc. 103*, 3926−3927.
53. Jencks, W. P. (1981) *Chem. Soc. Rev. 10*, 345−375.
54. Richard, J. P., and Jencks, W. P. (1984) *J. Am. Chem. Soc. 106*, 1383−1396.
55. Jencks, W. P. (1980) *Acc. Chem. Res. 13*, 161−169.
56. Kral, A. M., Diehl, R. E., deSolms, S. J., Williams, T. M., Kohl, N. E. and Omer, C. A. (1997) *J. Biol. Chem. 272*, 27319−27323,
57. Dolence, J. M., Cassidy, P. B., Mathis, J. R. and Poulter, C. D. (1995) *Biochemistry 34*, 16687−16694.
58. Admiraal, S. J. and Herschlag, D. (1995) *Chem. Biol. 2*, 729−739.
59. Meagley, K. A., Admiraal, S. J. and Herschlag, D. (1996) *Proc. Natl. Acad. Sci. 93*, 8160−8166.
60. *NIST Critical Stability Constants of Metal Complexes Database 46* (1993) U. S. Department of Commerce.

61. King, H. L., Jr., and Rilling, H. C. (1977) *Biochemistry 16*, 3815−3819.
62. Brems, D. N., and Rilling, H. C. (1977) *J. Am. Chem. Soc. 99*, 8351−8352.
63. Vial, M. V., Rojas, C., Portilla, G., Chayet, L., Perez, L. M. and Cori, O. (1981) *Tetrahedron 37*, 2351−2357.
64. Chayet, L., Rojas, M. C., Cori, O., Bunton, C. A., and McKenzie, D. C. (1984) *Bioorg. Chem. 12*, 329−338.
65. Poulter, C. D. and Rilling, H. C. (1978) *Acc. Chem. Res. 11*, 307−313.
66. Cane, D. E. (1990) *Chem. Rev. 90*, 1089−1103.
67. Lesburg, C. A., Zhai, G., Cane, D. E. and Christianson, D. W. (1997) *Science 277*, 1820−1824.
68. Wendt, K. U., and Schulz, G. E. (1998) *Structure 6*, 127−133.
69. Park, H.-W., Boduluri, S. R., Moomaw, J. F., Casey, P. J., and Beese, L. S. (1997) *Science 275*, 1800−1804.
70. Long, S. B., Casey, P. J., and Beese, L. S. (1998) *Biochemistry 37*, 9612−9618.
71. Myers, L. C., Terranova, P., Ferentz, A. E., Wagner, G., and Verdine, G. L. (1993) *Science 261*, 1164−1167.
72. Myers, L. C., Verdine, G. L., and Wagner, G. (1993) *Biochemistry 32*, 14089−14094.
73. González, J. C., Peariso, K., Penner-Hahn, J. E., and Matthews, R. G. (1996) *Biochemistry 35*, 12228−12234.
74. Jarrett, J. T., Choi, C. Y., and Matthews, R. G. (1997) *Biochemistry 36*, 15739−15748.
75. LeClerc, G. M., and Grahame, D. A. (1996) *J. Biol. Chem. 271*, 18725−18731.
76. Sauer, K., and Thauer, R. K. (1997) *Eur. J. Biochem. 249*, 280−285.
77. Witter D. J., and Poulter C. D. (1996) *Biochemistry 35*, 10454−10463.
78. Wilker, J. J., and Lippard, S. J. (1995) *J. Am. Chem. Soc. 117*, 8682−8683.

BI992356X